

AD-A173 945

GEAR MESH COMPLIANCE MODELING(U) NATIONAL AERONAUTICS
AND SPACE ADMINISTRATION CLEVELAND OH LEWIS RESEARCH
CENTER M SAVAGE ET AL 1986 NASA-E-3230 NASA-TN-88843

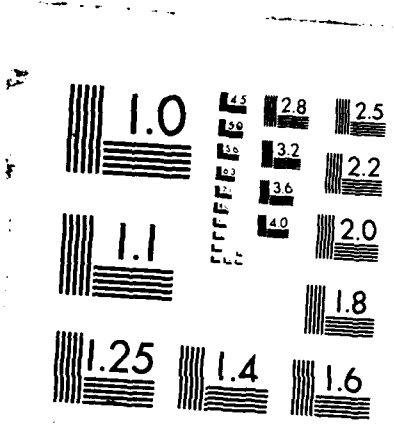
1/1

UNCLASSIFIED

F/G 13/9

NL





MICROCOPY RESOLUTION TEST CHART
NATIONAL BUREAU OF STANDARDS-1963-A

2

NASA
Technical Memorandum 88843

USAAVSCOM
Technical Report 86-C-28

AD-A173 945

Gear Mesh Compliance Modeling

M. Savage, R.J. Caldwell,
and G.D. Wisor
The University of Akron
Akron, Ohio

and

D.G. Lewicki
Propulsion Directorate
U.S. Army Aviation Research and Technology Activity—AVSCOM
Lewis Research Center
Cleveland, Ohio

Prepared for the
Rotary Wing Propulsion System Specialist Meeting
sponsored by the American Helicopter Society
Williamsburg, Virginia, November 12-14, 1986

DTIC
ELECTE
NOV 3 1986
S B D

FILE COPY



DISTRIBUTION STATEMENT A
Approved for public release
Distribution Unlimited



86 11 3 070

GEAR MESH COMPLIANCE MODELING

M. Savage, R.J. Caldwell, and G.D. Wisor
The University of Akron
Akron, Ohio 44325

and

D.G. Lewicki
Propulsion Directorate
U.S. Army Aviation Research and Technology Activity - AVSCOM
Lewis Research Center
Cleveland, Ohio 44135

SUMMARY

A computer model has been constructed to simulate the compliance and load sharing in a spur gear mesh. The model adds the effect of rim deflections to previously developed state-of-the-art gear tooth deflection models. The effects of deflections on mesh compliance and load sharing are examined. The model can treat gear meshes composed of two external gears or an external gear driving an internal gear. The model includes deflection contributions from the bending and shear in the teeth, the Hertzian contact deformations, and primary and secondary rotations of the gear rims. The model shows that rimmed gears increase mesh compliance and, in some cases, improve load sharing.

E-3230

NOMENCLATURE

- d_n dimensionless gear mesh deflection
 F_a radial tooth load, N (lb)
 F_b tangential tooth load, N (lb)
 F_t normal gear mesh force, N (lb)
 F_r tooth load fraction
 h moment arm to rim centroid, m (in)
 M resultant moment on rim, N·m (lb-in)
 m uniformly distributed rim support moment, N·m (lb-in)
 P pitch point
 R_0 inside rim radius for external gear, m (in); or outside rim radius for internal gear, m (in)
 S contact position, m (in)
 S_n normalized contact position



01st	
A-1	

- α rim rotation angle, deg
- ϕ pressure angle, deg

INTRODUCTION

Analytical models have been sought for the compliance of a gear mesh for over 60 years (ref. 1). One early model was that of Timoshenko (ref. 2). The "Timoshenko beam" is a trapezoidal cantilever which was formulated to model the deflection of a single gear tooth under load. Walker (ref. 3) improved this model with empirical equations to predict a tooth's deflection based on a series of laboratory deflection tests. He also suggested a method for modifying the tooth profile to compensate for the loaded deflection of the tooth so as to reduce the dynamic loads in the gear mesh. Weber (ref. 4) used strain energy to obtain analytical expressions for the tooth deflection based on an integration of the actual shape of the tooth. He also included the Hertzian contact deflection of mating teeth, and shear and bending deflections in a tooth and at its base.

This work was extended by Richardson (refs. 5 and 6) with experimental verification of the dynamic tooth loads caused by the tooth deflections. These methods have also been extended to include fillet deflections and have been adapted to digital computation by R. Cornell (refs. 7 and 8) in a program which predicts the dynamic loading on the tooth and its deflection in the mesh under steady-state running conditions.

All of these methods assume that the deflection of a tooth is caused only by its own load and that the base of the tooth is mounted in a rigid rim. In this work (refs. 9 and 10), the deflection model of a tooth has been extended to include rim bending effects at the base of the tooth on either an external or internal gear.

COMPLIANCE MODEL

Figure 1 shows the mesh region for a pair of external gears. The bottom gear is the pinion and is the driving gear. The line of action is shown for clockwise rotation of the pinion. In the position shown, the load is transferred from the pinion to the gear through a single tooth on the pinion to a single tooth on the gear. This will be referred to as the single contact region in the discussion to follow.

If the center of the driven gear is held fixed and a torque is applied at the center of the driving gear, the teeth in contact and the bodies of both gears will deform. This condition yields an angular displacement of the center of the driving gear relative to the fixed frame of reference at the center of the driven gear. The relative angular displacement of the gears can be converted to a linear displacement along the line of action. The total relative displacement of the driving gear with respect to the driven gear along the line of action is defined as the mesh deflection. Dividing this by the base pitch produces the dimensionless mesh deflection, d_n . Note that the mesh deflection is not the displacement of the point of contact of the gear tooth.

In the single contact region, the full load is carried by one tooth pair. In the two double contact regions which occur before and after the single contact region, the load is shared by the two mating tooth pairs in contact. In the double contact regions, the tooth load fraction, f_r , is defined as the load transferred by a tooth pair divided by the total load.

The distance from the pitch point, P , to a point of contact is called the contact position, S (fig. 2). The contact position is negative as the tooth pair approaches the pitch point as shown in figure 2 and positive as the tooth pair recedes from the pitch point. The contact position is divided by the base pitch to obtain the normalized contact position, S_n , against which the mesh properties are plotted. This distance is measured in space along the line of action and can be related to positions on both the pinion and gear teeth.

Figure 3 shows an external gear tooth with a rim base. The present gear tooth deflection model treats the tooth as though it were loaded with a tangential force, F_b , and a radial force, F_a , applied at the point at which the line of action crosses the tooth centerline. Tooth bending and shear are caused by the tangential force. A small compressive deflection is a result of the radial force component. A Hertzian deflection also exists for the mating teeth. These deflections are all found by the methods of reference 8. All tooth deflections are resolved into components which are directed along the line of action.

In this work, the gear deflection model is expanded to include rim effects (refs. 9 and 10). The moment on the rim is shown in figure 4(a) as a tangential force component, F_b , and lever arm, h . This concentrated moment is assumed to be supported by a uniformly distributed moment, m , around the rim, and a reaction, F_b , at the base of the lever arm. In figure 4(b), the positive and negative rim bending moment, M , which results from this loading is plotted versus circumferential position in the rim. This yields a very compliant model for the rim deflection and thus serves as an upper bound for the mesh deflections including rim effects. The rigid body model serves as a lower bound for these mesh deflections.

The rim deflection model is a simplified model for the loading and deflections in a rimmed gear. A gear with a rim may be constructed with a splined connection to the transmission housing, a thin torque tube shaft, spokes to a solid hub or with a series of fasteners to a housing or hub. In these and other specific constructions, the rim stiffness is influenced by its particular attachment's stiffness. Since most of these are discrete, the total stiffness will fluctuate as the gear rotates. Right at a spoke or attachment point, the stiffness will be greater than it is at midspan between adjacent spokes. Each attachment construction will support the applied moment, $h * F_b$, with a series of discrete moments or a continuously varying moment around the rim in front of and behind the applied moment. In most cases, the rim moment will drop to zero in less than a half rim as assumed in the model. This reduces the actual rim strain energy from that presented here. Thus the model is considered to be an upper bound for the rim deflections in an actual gear.

The rotational deformation of the rim, which varies along its circumference, is found from the bending strain energy in the rim (ref. 11). Shear and axial strain energies are ignored due to the high circumferential length to radial thickness ratio of the rim. The rim thickness is taken to be the root mean cube of the varying rim thickness including the teeth to average the tooth

stiffening effects on the rim, and the neutral axis of the rim is taken to be its centroid. This rotational deformation is converted into a translation of the tooth centerline along the line of action for inclusion in the total mesh deflection. When the teeth are in the double contact regions as shown in figure 5, each contact load produces deflections at both loaded teeth on both gears. For each load, each tooth has its own rim rotation, α , rim lever arm, h , and pressure angle, ϕ , for conversion into a deflection along the line of action.

LOAD SHARING

In the double contact region shown in figure 5, the tooth load fractions of the mating tooth pairs must produce equal mesh deflections. Since the mesh deflection is the total relative displacement of the pinion with respect to the gear along the line of action, this displacement must be the same for all tooth pairs in contact. Unequal mesh deflections of mating tooth pairs imply a discontinuity in the gear bodies.

The load fractions are determined by an iteration procedure which changes the load fractions from an initial guess of 50 percent each until the two load fractions are found which cause the mesh deflections to be equal. When no rim bending is present, the determinations of the deflections of each of the four teeth in contact are independent. When rim bending is present, each tooth in contact has an additional rim deflection caused by the load on the other tooth on the same gear.

Figures 6 and 7 are load sharing and deflection plots for a 4:1 gear ratio with 24 teeth on the pinion and 96 teeth on the gear. The Hertzian component of deflection is nonlinear with load. Thus the plots are slightly dependent on load although presented in terms of dimensionless parameters. All plots presented in this paper were obtained for eight diametral pitch steel gears with a face width of 0.016 m (0.625 in) and a transmitted load of 4000 N (900 lb). These gears have a maximum Hertzian tooth contact pressure of about 1 GPa (150 000 psi).

For a 24 to 96 tooth solid body gear speed reduction, figure 6 shows the classic load sharing plot. This plot is nearly symmetric, with the full load carried in the central single contact region and partial loads carried in the two double contact regions to either side of the single contact region. In the double contact region, the load fraction is the smallest at the beginning and end of contact and the largest just before and after the single contact region.

Figure 7 shows the mesh deflections caused by these tooth loads. The mesh deflections are the largest in the single contact region where the full load is carried by a single tooth pair. In the double contact region, the mesh deflection drops to about 60 percent of that in the single contact region. The reason that this deflection is greater than 50 percent is the variation in tooth pair stiffness along the line of action. An individual tooth pair is most stiff in the center of the single contact region, where both teeth are loaded near their respective pitch circles.

Although these deflections do not vary linearly as the tooth pair moves through the mesh, they are equal to the deflections one base pitch away at the second tooth pair in the mesh. It is this equality of deflections which is

used to obtain the load fraction at each contacting tooth pair in the double contact region.

EXAMPLES

By adding a rim to the larger gear with 96 teeth, the load sharing and deflection plots change to those of figures 8 and 9. The rim thickness chosen for this presentation is twice the whole depth of the teeth. Comparison of figures 6 and 8 shows that the rim deflections decrease the load on the pinion tooth as it enters the mesh in contact with the tip of a gear tooth. Rim effects also increase the load fraction on the pinion tooth as it leaves the single contact region in contact with the rimmed gear tooth near its base. The sum of the two load fractions one base pitch apart is still one. It is interesting to note that the greater flexibility of the rimmed gear teeth reduces the initial load on the pinion tooth where it enters the mesh just as tip relief on the gear teeth can.

Note that the cases presented here are for rimmed driven gears only. If a rim is added to the driving pinion also, the total mesh deflection increases but the load sharing returns to a more symmetric case and the load fraction in the double contact region is more nearly constant. If a rim is present on the driving pinion only, then the reverse load sharing effect of the first case is produced. The pinion tooth would see a larger share of the load as it entered the mesh and a smaller fraction of the load after it left the single contact region.

Figure 9 shows the mesh deflection which corresponds to the load sharing with the effects of rim flexibility on the driven gear teeth. The mesh deflection shows a gradual stiffening as the contact progresses along the line of action toward the base of the more flexible gear teeth. As before, the deflections separated by one base pitch are equal. However, this deflection decreases as one progresses through the two double contact regions. It can be noted that this stiffening also causes the load fraction in the second tooth pair to be higher than that in the first tooth pair in the load sharing plot of figure 8.

A second major difference between these deflections and those for the same gears with solid bodies is the overall deflection magnitudes. The deflections of figure 9 are roughly double those of figure 7. This means that the mesh with a single rim on the loaded gear can be at least twice as compliant as the mesh with two solid bodies. In a transmission which has parallel load paths, this additional compliance can make the rimmed teeth less sensitive to manufacturing dimensional variations from a load sharing viewpoint.

A major reason for rims in aircraft gearing is weight savings. One concern in using a rim is the design trade off between the benefits of lower weight and greater gear tooth flexibility and the penalty of higher gear tooth rim bending stress. As the rim below the tooth is made thinner, the maximum bending stress at the root of the tooth shifts from the tooth to the rim between the teeth and increases in value (ref. 12). Rimmed gear designs must also consider this stress to avoid bending fatigue failure of the gear rim.

Figures 10 through 13 are for contact between a pinion with 24 teeth and an internal gear with 96 teeth. These plots compare the same two situations

of a rigid body gear and a gear with a flexible rim. To avoid tip interference, the addendum ratio of the internal gears is reduced to 0.9 from the standard value of 1.0 used for the external gears. The dedendum ratio for all gears is 1.35 for grinding clearance. The rim thickness for the internal gear is kept at two times the whole depth of the external teeth for comparison purposes.

Figures 10 and 11 show the load sharing and mesh deflections for the 4:1 ratio with an internal gear. Due to the higher contact ratio relative to that for an external gear mesh, the single contact region is smaller than that of figure 6. The internal tooth is stiffer due to its wider base and shorter height, but its tip is closer to its base circle than that of an external tooth. This inversion of the tooth decreases the pressure angle on the tooth and causes the normal load on the tooth to have a greater moment arm. The increased leverage offsets the increased stiffness of the tooth to yield load sharing and mesh deflection plots surprisingly similar to those of the external gear ratio of figures 6 and 7. Other than the contact ratio increase, the only noticeable difference between the mesh deflection curve for the internal gear of figure 11 and that for the external gear of figure 7 is a slight increase in deflection for the internal gear mesh in the single contact region only.

By adding the rim to the internal gear, the load sharing and mesh compliance plots of figures 12 and 13 are produced. In the load sharing plot of figure 12, the pinion tooth load shows the same trend as that for the external gear in figure 8. Both the load sharing and mesh deflection curves are very similar to those for the external gear case, as with the solid body case. The only differences are the increase in contact ratio and the small increase in mesh deflection in the single contact region.

The advantages of rimmed construction for the external gear are also present for the internal gear. For example, consider an internal - external steel gear speed reduction of 4:1 with 24 teeth on the external pinion, 96 teeth on the internal gear, a diametral pitch of 8, a face width of 16 mm (0.625 in), an outside rim radius of 168 mm (6.614 in.) and a driving torque of 150 N-m (1350 lb-in) applied to the pinion. The maximum static Hertz contact pressure for these gears is 1 GPa (146 ksi) at the tip of the gear tooth while the maximum bending stress is 0.23 GPa (33 ksi) in the root of the pinion tooth for the load at the top of single tooth contact. The base pitch of this gear set is 9.37 mm (0.369 in). The rim model predicts a maximum mesh deflection of 33.7 μm (0.00133 in) and an initial mesh deflection of 28 μm (0.00111 in). The rigid body gear model predicts mesh deflections of 17 μm (0.00066 in) and 11 μm (0.00044 in) for these two deflections. An additional effect of the rim is to drop the initial load fraction from 0.43 to 0.25. This drops the initial tooth load from 1700 N (390 lb) to 1000 N (225 lb). The effects of gear rim flexibility has doubled the mesh deflection and reduced the initial load to 60 percent of the value for the solid bodied gears.

SUMMARY OF RESULTS

A model for the load sharing and deflections in a spur gear mesh has been presented. This model adds the effects of rim deflections to previously developed state-of-the-art gear deflection models. Internal as well as external gears can be modeled with rims or with solid bodies. The rimmed construction model assumes a soft continuous support. By using the solid body analysis as

a lower bound for the mesh compliance and the rim analysis as an upper bound for the mesh compliance, reasonable approximations can be obtained for the compliance in a spur gear mesh. By modeling the internal gear as well as the external gear, analyses can be performed for the load sharing and mesh compliances in a planetary transmission.

The model showed that a rim on the larger output gear in a spur gear mesh can improve the load sharing characteristics of the mesh. The improvement was shown for both an external output gear and an internal output gear of the same size. The load sharing improvement reduced the driving pinion tooth load fraction as the tooth entered the mesh. One effect of this reduced initial load fraction is a potential reduction in dynamic loading on the tooth. A second improvement is an increase in the total mesh compliance which can reduce tolerance sensitivity in parallel path power transmissions.

REFERENCES

1. Furrow, R.W. and Mabie, H.H., "The Measurement of Static Deflection in Spur Gear Teeth," *Journal of Mechanisms*, 5, (2), 1970, pp. 147-168.
2. Tomoshenko, S. and Baud, R.V., "Strength of Gear Teeth is Greatly Affected by Fillet Radius," *Automotive Industries*, 55, (4), 1926, pp. 138-142. (See also *Mechanical Engineering*, 48, (11), 1926, pp. 1105-1109).
3. Walker, H., "Gear Tooth Deflection and Profile Modification," *The Engineer*, 166, (4318), 1938, pp. 409-412; 166, (4319), 1938, pp. 434-436; 170, (4414), 1940, pp. 102-104.
4. Weber, C., "The Deformation of Loaded Gears and the Effect on Their Load Carrying Capacity," Department of Scientific and Industrial Research, Sponsored Research, (Germany) Report No. 3, London, England, 1949.
5. Richardson, H.H., "Static and Dynamic Load, Stress, and Deflection Cycles in Spur-Gear Systems," Sc.D. Thesis, Dept. of Mech. Eng., MIT, Cambridge, MA, 1958.
6. Richardson, H.H., "Dynamic Loading of High Speed Gearing," in *Transactions of the Seventh Conference on Mechanisms*, Penton Publishing, Cleveland, OH, 1962, pp. 146-160.
7. Cornell, R.W. and Westervelt, W.W., "Dynamic Tooth Loads and Stressing for High Contact Ratio Spur Gears," *Journal of Mechanical Design*, 100, (1), 1978, pp. 69-76.
8. Cornell, R.W., "Compliance and Stress Sensitivity of Spur Gear Teeth," *Journal of Mechanical Design*, 103, (2), 1981, pp. 447-459.
9. Wisor, G.D., "Load Sharing in a Compliant Gear Mesh," M.S. Thesis, Dept. of Mech. Eng., The Univ. of Akron, 1985.
10. Caldwell, R.J., "Load Sharing and Elastic Deformation in a Gear Mesh," M.S. Thesis, Dept. of Mech. Eng., The Univ. of Akron, 1986.

11. Seely, F.B. and Smith, J.O., Advanced Mechanics of Materials, 2nd ed., Wiley, New York, 1952.
12. Drago, R.J., "An Improvement in the Conventional Analysis of Gear Tooth Bending Fatigue Strength," Amer. Gear Manufacturing Association, Technical Paper P229.24, Oct. 1982.

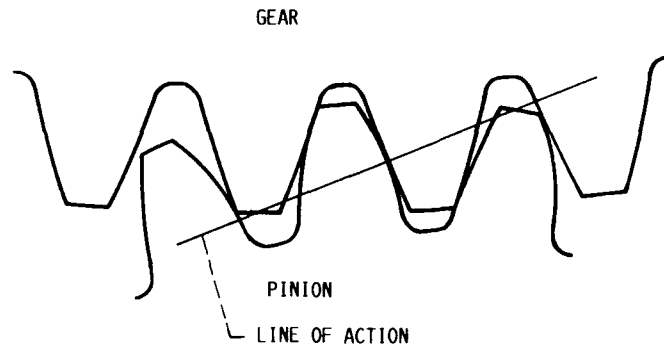


FIGURE 1.- A 24:96 EXTERNAL GEAR REDUCTION WITH THE TEETH IN THE SINGLE CONTACT REGION.

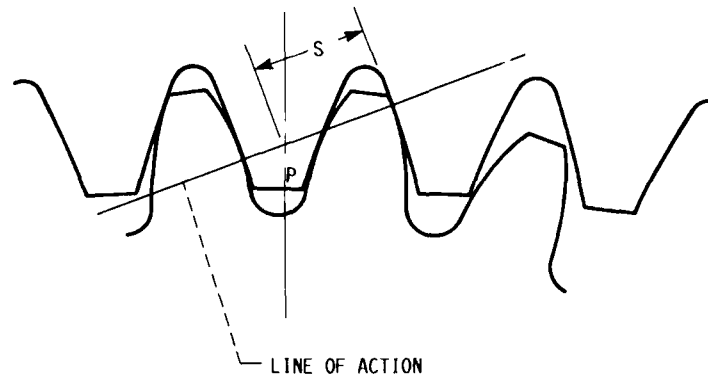


FIGURE 2.- A 24:96 INTERNAL GEAR REDUCTION WITH THE TEETH IN THE DOUBLE CONTACT REGIONS.

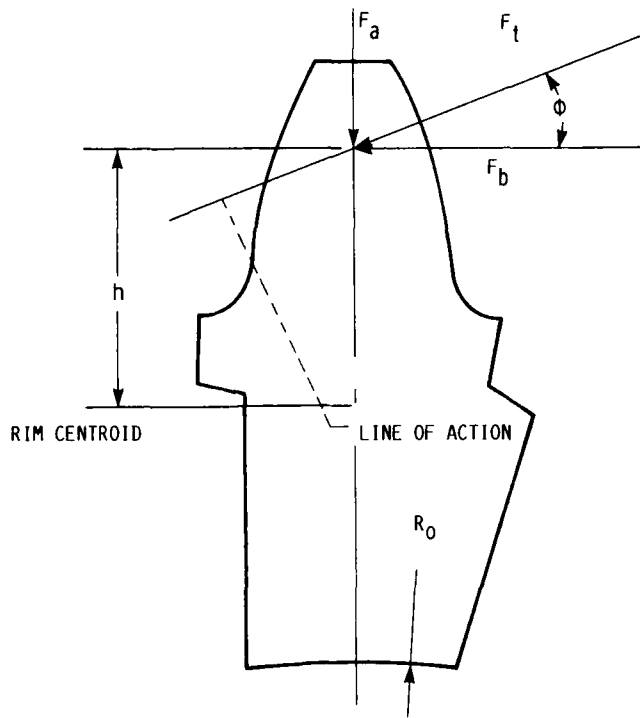


FIGURE 3.- A SINGLE TOOTH FROM A 24 TOOTH GEAR WITH A RIM.

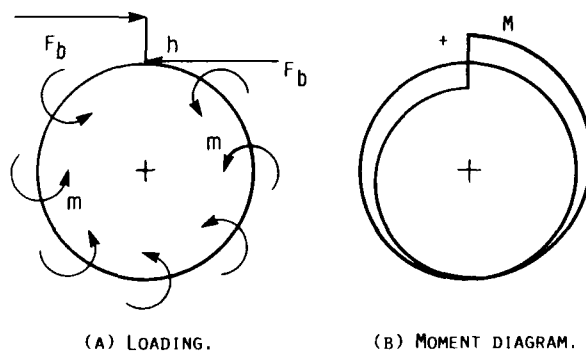


FIGURE 4.- RIM BENDING MODEL.

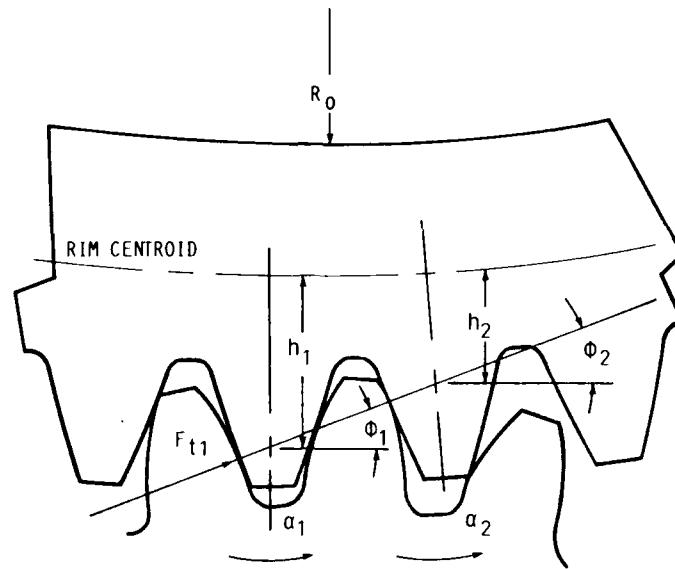


FIGURE 5.- A 24:96 EXTERNAL GEAR REDUCTION WITH THE TEETH IN THE DOUBLE CONTACT REGIONS.

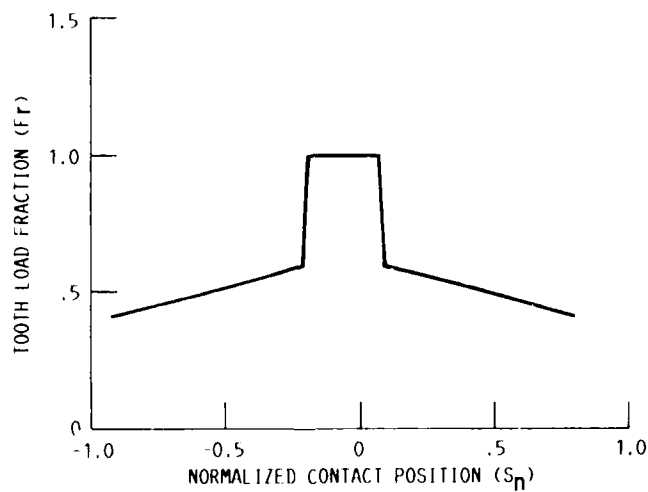


FIGURE 6.- LOAD SHARING PLOT FOR A 24:96 EXTERNAL GEAR REDUCTION WITH SOLID BODIES.

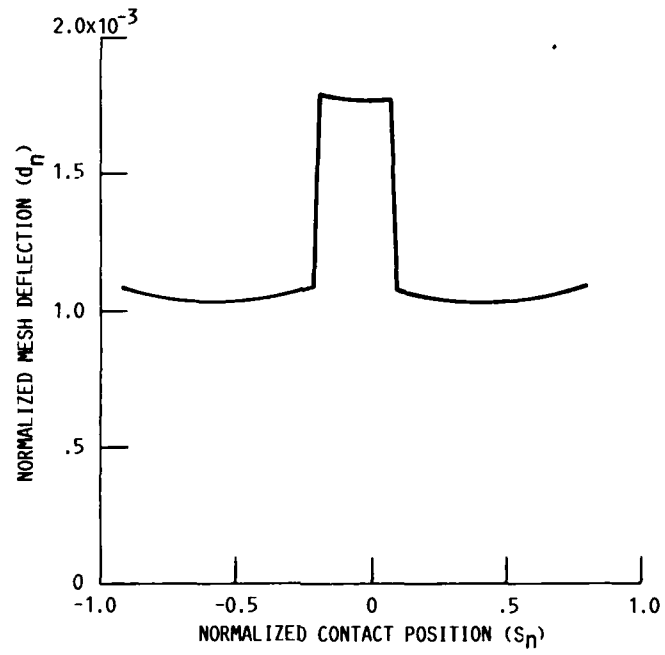


FIGURE 7.- MESH DEFLECTION PLOT FOR A 24:96 EXTERNAL GEAR REDUCTION WITH SOLID BODIES.

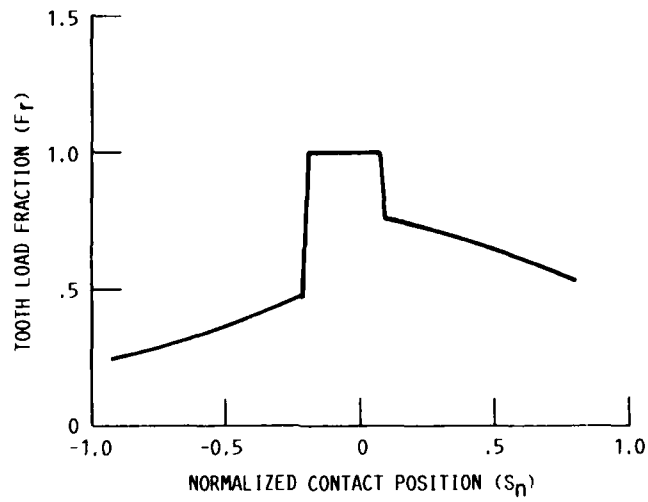


FIGURE 8.- LOAD SHARING PLOT FOR A 24:96 EXTERNAL GEAR REDUCTION WITH A SOLID PINION BODY AND A GEAR RIM.

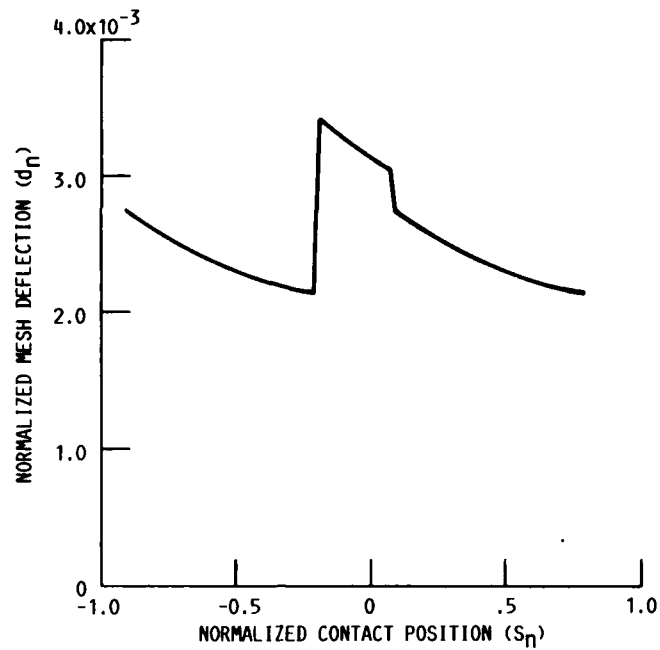


FIGURE 9.- MESH DEFLECTION PLOT FOR A 24:96 EXTERNAL GEAR REDUCTION WITH A SOLID PINION BODY AND A GEAR RIM.

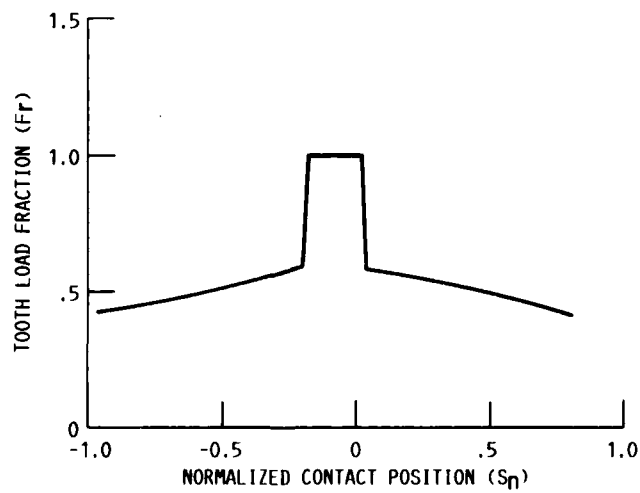


FIGURE 10.- LOAD SHARING PLOT FOR A 24:96 INTERNAL GEAR REDUCTION WITH SOLID BODIES.

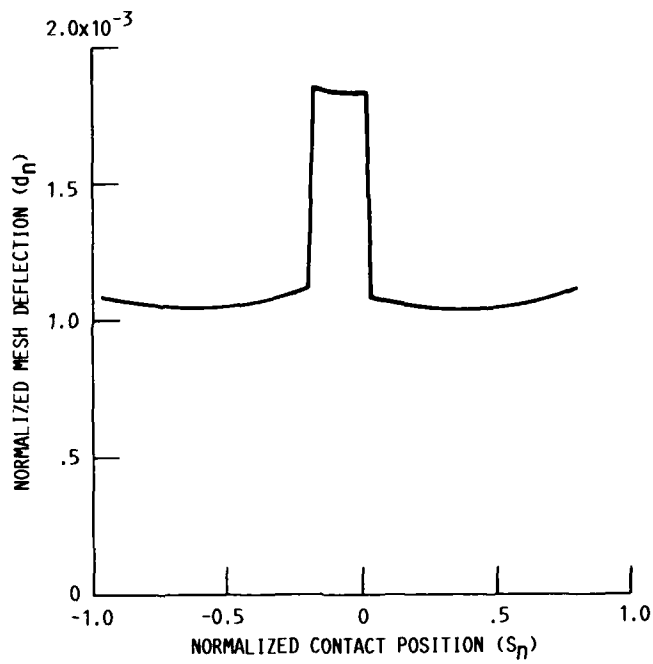


FIGURE 11.- MESH DEFLECTION PLOT FOR A 24:96 INTERNAL GEAR REDUCTION WITH SOLID BODIES.

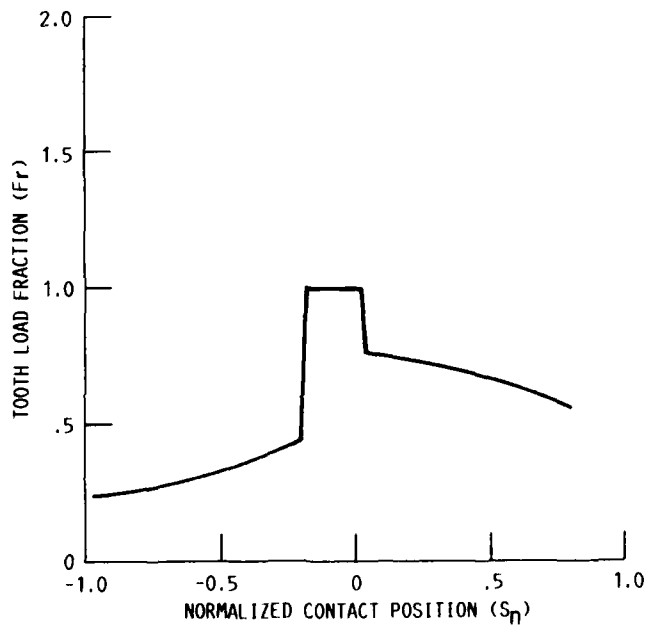


FIGURE 12.- LOAD SHARING PLOT FOR A 24:96 INTERNAL GEAR REDUCTION WITH A SOLID PINION BODY AND A GEAR RIM.

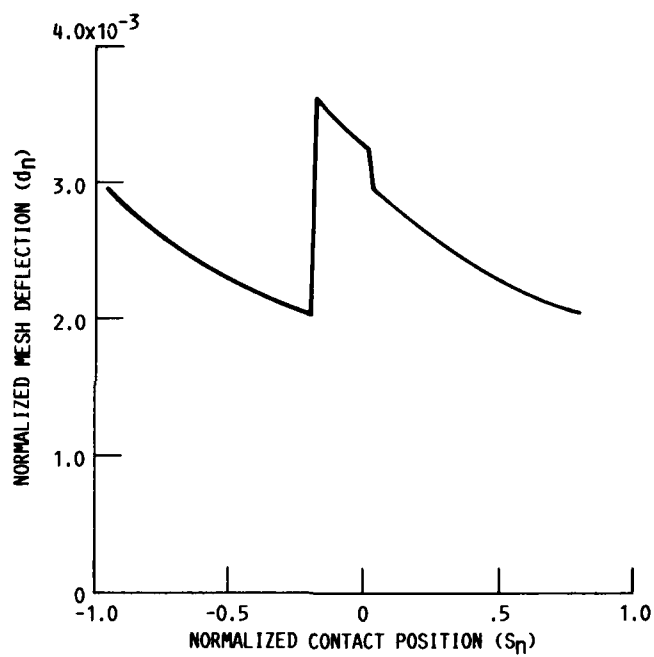


FIGURE 13.- MESH DEFLECTION PLOT FOR A 24:96 INTERNAL GEAR REDUCTION WITH A SOLID PINION BODY AND A GEAR RIM.

1. Report No. NASA TM-88843 USAAVSCOM-TR-86-C-28		2. Government Accession No.		3. Recipient's Catalog No.	
4. Title and Subtitle Gear Mesh Compliance Modeling				5. Report Date	
				6. Performing Organization Code 505-62-51	
7. Author(s) M. Savage, R.J. Caldwell, G.D. Wisor, and D.G. Lewicki				8. Performing Organization Report No. E-3230	
				10. Work Unit No.	
9. Performing Organization Name and Address NASA Lewis Research Center and Propulsion Directorate, U.S. Army Aviation Research and Technology Activity - AVSCOM, Cleveland, Ohio 44135				11. Contract or Grant No.	
				13. Type of Report and Period Covered Technical Memorandum	
12. Sponsoring Agency Name and Address National Aeronautics and Space Administration Washington, D.C. 20546 and U.S. Army Aviation Systems Command, St. Louis, Mo. 63120				14. Sponsoring Agency Code	
15. Supplementary Notes Prepared for the Rotary Wing Propulsion System Specialist Meeting, sponsored by the American Helicopter Society, Williamsburg, Virginia, November 12-14, 1986. M. Savage, R.J. Caldwell, and G.D. Wisor, The University of Akron, Akron, Ohio 44325 (work performed under NASA Grant NAG3-55); D.G. Lewicki, Propulsion Directorate, U.S. Army Aviation Research and Technology Activity - AVSCOM, Lewis Research Center.					
16. Abstract A computer model has been constructed to simulate the compliance and load sharing in a spur gear mesh. The model adds the effect of rim deflections to previously developed state-of-the-art gear tooth deflection models. The effects of deflections on mesh compliance and load sharing are examined. The model can treat gear meshes composed of two external gears or an external gear driving an internal gear. The model includes deflection contributions from the bending and shear in the teeth, the Hertzian contact deformations, and primary and secondary rotations of the gear rims. The model shows that rimmed gears increase mesh compliance and, in some cases, improve load sharing.					
17. Key Words (Suggested by Author(s)) Gears; Compliance; Deflections; Load sharing; Rims			18. Distribution Statement Unclassified - unlimited STAR Category 37		
19. Security Classif. (of this report) Unclassified		20. Security Classif. (of this page) Unclassified		21. No. of pages	22. Price*

END

12-86

DTIC